THE JOURNAL OF PHYSICAL CHEMISTRY B

Article

pubs.acs.org/JPCB

Dynamic Turn Conformation of a Short Tryptophan-Rich Cationic Antimicrobial Peptide and Its Interaction with Phospholipid Membranes

Matthew Nichols,[†] Miljan Kuljanin,[†] Mostafa Nategholeslam,[§,‡] Tuan Hoang,[†,‡] Shaghayegh Vafaei,[§,‡] Bruno Tomberli,[§,‡,∥] C. G. Gray,[§,‡] Lillian DeBruin,[†] and Masoud Jelokhani-Niaraki*[,†,‡]

[†]Department of Chemistry, Wilfrid Laurier University, 75 University Avenue West, Waterloo, Ontario N2L 3C5, Canada

[§]Department of Physics, University of Guelph, MacNaughton Building, Guelph, Ontatrio N1G 2W1, Canada

[‡]Biophysics Interdepartmental Group, University of Guelph, 50 Stone Road East, Guelph, Ontario N1G 2W1, Canada

Supporting Information

ABSTRACT: Cationic antimicrobial peptides are promising sources for novel therapeutic agents against multi-drug-resistant bacteria. HHC-36 (KRWWKWWRR) is a simple but effective antimicrobial peptide with similar or superior activity compared with several conventional antibiotics. In this biophysical study, unique conformational properties of this peptide and some of its analogs as well as its interaction with lipid membranes are investigated in detail. Circular dichroism (CD) and molecular dynamics modeling studies of HHC-36 in different environments reveal a dynamic amphipathic structure composed of competing turn conformations with free energies lower than that of the unfolded state, implying a strong influence of tryptophan interactions in formation of the turns. CD spectra and gel electrophoresis also show strong evidence of self-association of this peptide in aqueous milieu and interaction with both neutrally and negatively charged lipid membrane systems. Isothermal titration calorimetry and acrylamide fluorescence quenching experiments emphasize the preference of HHC-36 for negatively charged vesicles. In addition, dye leakage experiments suggest that this peptide functions through a surface-associated mechanism with weak lytic activity against bacterial model membranes.

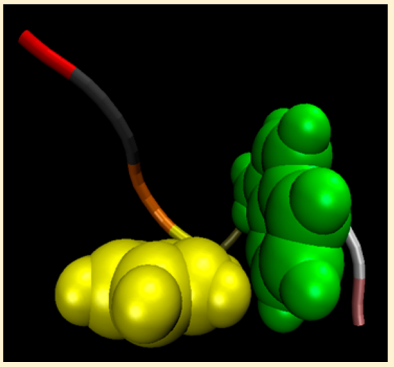

INTRODUCTION

Antimicrobial peptides have been emerging as new potential agents against multi-drug-resistant bacteria that are responsible for a growing number of infections. The need for effective antimicrobial agents is an urgent issue; however, in the past few decades, only a few types of novel broad-spectrum antibiotics were produced commercially.[1] Cationic antimicrobial peptides (CAPs) are produced by virtually all species of life for direct antibiotic activity or for their roles in the innate immune response.[2] These peptides are a promising source for new antibiotics, which could also be used synergistically with conventional antibiotics against multi-drug-resistant microbial infections.

HHC-36 (KRWWKWWRR; M_w = 1488 Da; pI = 12.3) is a synthetic nonameric CAP, designed through neural network analysis,[3] which shows a broad-spectrum activity against multi-drug-resistant strains of both Gram-positive and -negative bacteria and minimal toxicity against mammalian erythrocytes. In initial in vitro testing against some multi-drug-resistant bacteria, HHC-36 had activities equal to or greater than commonly used conventional antibiotics, such as tobramycin and ciproflaxin.[3] HHC-36, and another synthetic peptide HHC-10 (KRWWKWIRW), were selected through a predictive computer software in conjunction with microarray synthesis of 100 000 peptides.[3] This peptide is among the smallest reported effective antimicrobial peptides, which makes it appealing to pharmaceutical companies as a potential therapeutic agent.[4] The structural properties and mechanism of biological activity of this peptide have not been previously investigated.

CAPs are characterized by their relatively short length, possession of an excess of positively charged amino acids, and general amphipathicity.[5] Bacterial membranes typically possess an excess negative charge in contrast with more neutral mammalian membranes.[6] CAPs are therefore thought to be generally selective toward the negatively charged bacterial membranes through long-range electrostatic interactions. In addition to this inherent selectivity, cationic peptides offer other advantages over conventional antibiotic treatments. For example, their antibacterial action is faster and allows less opportunity for the development of bacterial resistance.[4] Antimicrobial peptides act through a variety of different mechanisms and multiple cellular targets. These mechanisms can include membrane lysis, transmembrane pore formation, septum prevention, interactions with membrane bound proteins, and internalization to interact with nucleic acids and proteins.[7−10]

Received: September 29, 2013
Revised: November 3, 2013
Published: November 6, 2013

dx.doi.org/10.1021/jp4096985 | J. Phys. Chem. B 2013, 117, 14697−14708

To understand the mechanism of biological activity of HHC-36, in this study, we investigated the unique conformational properties and interactions of this peptide with model bacterial and mammalian membranes.

MATERIALS AND METHODS

Chemicals. Fmoc-protected amino acids, resin supports, coupling reagents, and solvents used for peptide synthesis were from either Advanced ChemTech or Novabiochem-EMD Biosciences. Phospholipids were from Avanti Polar. Calcein (sodium salt) was from Alfa Aesar. All other chemicals were from Sigma.

Peptide Synthesis and Purification. HHC-36, its aromatic substitution analogs, and HHC-10 were synthesized by solid-phase Fmoc chemistry procedures on Wang resin, as previously described.[11] In brief, HCTU, HOBt, and DIPEA in DMF were used to activate the C-terminus of amino acids, and a 20% piperidine solution in DMF was utilized for Fmoc deprotection. The peptides were purified by a Waters 600E RP-HPLC (reversed-phase high-performance liquid chromatography) system. Concentration of the peptides in aqueous solutions was corrected using Trp absorption at 280 nm.[12] Final purity of the peptides was ≥95% and confirmed by both analytical RP-HPLC and electrospray mass spectrometry (Waters ZQ4000). Luna C5 (Phenomenex) analytical and semipreparative RP-HPLC columns were used.

Preparation of Large Unilamellar Vesicles. Chloroform stock solutions of lipids POPC, POPC/POPG, and POPE/POPG (both at 3:1 molar ratio) were dried under a mild nitrogen stream in a round-bottomed flask forming a film, further dried under reduced pressure overnight. The dry lipid film was then rehydrated and extruded through a 100 nm filter in a mini extruder (Avanti Polar) to give LUVs.[13] These lipid systems were used in spectroscopic and calorimetric studies. The PE/PG system could not be used in CD measurements due to precipitation at high peptide−lipid molar ratios.

LUVs for dye-leakage experiments were prepared by rehydration of phospholipids in 70 mM calcein solutions containing 10 mM Tris at pH 7.4, as previously described.[14] Nonencapsulated calcein was removed from vesicles by a sephadex G-75-50 (Sigma) size-exclusion chromatography column (14 × 1.3 cm) equilibrated with 10 mM Tris buffer containing 150 mM NaCl at pH 7.4. The final concentration of lipids was measured by the Bartlett assay.[14]

SDS-PAGE Analysis. The association of HHC-36 peptide was analyzed using the SDS-PAGE technique. Samples were incubated in the sample loading buffer containing 70 mM SDS and heated to 85 °C for 5 min prior to gel loading. A 16% resolving gel was used to capture the migration of small peptides. SDS-PAGE gels were stained with Coomassie Brilliant Blue R-250. Band intensities of HHC-36 on gel were analyzed using the ImageLab software. The intensity of peptide band on SDS-PAGE was reported as the volume intensity relative to that of the 4 kDa band in the SeeBlue Plus2 prestained standard (Invitrogen).

Molecular Dynamics Simulations. A series of all-atom molecular dynamics simulations were applied to the HHC-36 peptide in buffer at different temperatures. In these atomistic simulations, HHC-36 was located in a water-box consisting of 9258 TIP3P water molecules and 7 sodium and 12 chloride ions. Pair interactions between atoms were provided by the CHARMM36 force field.[15] The imbalance in number of ions was to compensate for the positive net charge on the peptide (+5e), hence rendering the whole box electrically neutral. The simulations were run under NPT conditions (constant particle number, pressure, and temperature) with pressure set at 1.00 atm. To avoid bias toward any particular fold, a fully stretched structure of HHC-36, with a distance 45.840 Å between the first and ninth (last) α-carbon atoms, was used in constructing the initial configuration for simulations. A cubical water-box with initial dimensions of 60 × 60 × 60 Å^3 was constructed around this initial structure using the above-mentioned number of water molecules and ions. The constructed simulation box, containing the peptide, was run at 290 (124.5175 ns), 300 (107.712 ns), 320 (107.2815 ns), 330 (110.3645 ns), and 340 K (108.1405 ns). A much longer run time was applied at 310 K (∼1600 ns) to better estimate the physiologically relevant structure of the molecule. The final peptide structure obtained at 310 K was used as a reference for comparison of the structures obtained at other temperatures. Longer run-time simulations were also performed at 278 (395.6705 ns) and 350 K (320.1955 ns) (the minimum and maximum temperatures used in these simulations). These simulation times were deemed sufficient, given recent work for peptides of this size showing a folding time on the order of 100 ns.[16] A time step of length 2.00 fs was used for these simulations with all chemical bond lengths involving a hydrogen kept constant. Electrostatic interactions were handled using particle mesh Ewald method. Electrostatic and van der Waals forces were smoothly cut off at pair-distances of 10 Å. Pressure was kept at 1.00 atm using the Nosé−Hoover method, and temperature was kept at the given value for each series of simulations using Langevin dynamics, with a damping coefficient of 5/ps.

For the peptide-membrane simulations, a bilayer with 64 phospholipid molecules in each leaflet was composed. The bilayer was hydrated with layers of water on both sides and pre-equilibrated in each case. In the cases of mixed membranes (POPC/POPG and POPE/POPG), 16 POPG and 48 POPC or POPE molecules were used in each leaflet. The peptide molecule, together with a proper number of water molecules, was then added on top of each equilibrated hydrated membrane system. These additions led to systems containing 11 592, 11 881, and 13 531 water molecules with the POPC, POPC/POPG, and POPE/POPG membranes, respectively. In addition, an appropriate number of Na^+ and Cl^- ions was added to all three systems to give a physiological salt concentration of ∼150 mM and also render the systems electrically neutral. The resulting combined peptide−lipid systems were then further equilibrated at 310 K and 1 atm for 5 (POPE/POPG system) and 10 ns (POPC and POPC/POPG systems). Longer equilibration time was needed for systems containing POPC, as POPC membranes generally take more time to stabilize. For each lipid system, the HHC-36 molecule was initially kept at a distance of 55 Å from the center of mass of the membrane and along the direction normal to the surface of the membrane. The peptide was then moved toward the membrane at a velocity of 5 Å/ns, for a duration of 7 ns, until it reached a distance of 20 Å from the center of mass of the membrane. The peptide was then kept at this distance for 0.5 ns and then brought back to the initial position at 55 Å from the center of mass of the membrane, also at a velocity of 5 Å/ns. The peptide was kept for another 0.5 ns at this location, and then the whole cycle was repeated. Each cycle took 15 ns, and during this period the peptide experienced the membrane effect at various levels, depending on its distance from the membrane. At a distance of 20 Å, the peptide is well within the

dx.doi.org/10.1021/jp4096985 | J. Phys. Chem. B 2013, 117, 14697−14708

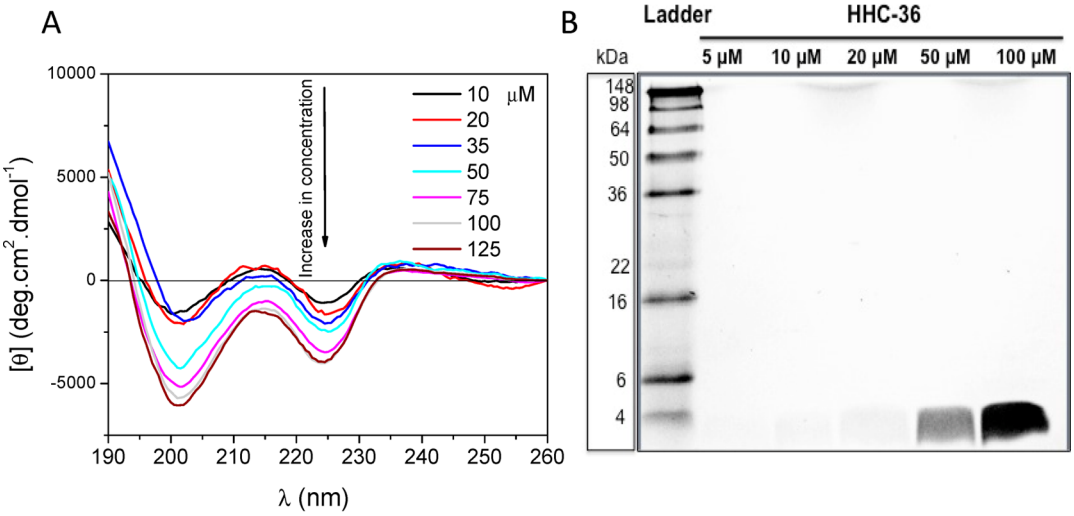

Figure 1. (A) Concentration dependence CD spectra of HHC-36 in buffer at 25 °C. Refer to the Materials and Methods section for experimental details. (B) SDS-PAGE analysis of HHC 36 self-association. Peptides were loaded with the final concentration of 5, 10, 20, 50, and 100 μM. SeeBlue Plus2 prestained standard was used as ladder (left line in panel B). Gel was run at 105 V for 70 min, stained, and visualized with Coomassie R-250 dye. For more details, refer to the Materials and Methods section.

phospholipid head-groups, while at 55 Å it is outside the range of interaction with membrane surface.

Preparation of the initial configuration of these systems as well as (part of) the final analysis was done using the VMD molecular visualization program (versions 1.8.7 and 1.9.1).[17] The simulations were performed using the NAMD (version 2.8),[18] on computational facilities provided by Compute Canada.

Instrumentation and Measurement Methodology. All CD spectra were measured on an Aviv 215 spectropolarimeter (Aviv Biomedical) in 10 mM Tris buffer containing 150 mM NaF at pH 7.4. NaF was used instead of NaCl to reduce the chloride absorption in measurements below 200 nm. CD spectra in both salts were comparable. Ellipticities are reported as mean residue ellipticity, $[\theta]$.

ITC measurements were performed on a VP-ITC microcalorimeter (MicroCal) at 37 °C. All solutions were degassed under reduced pressure with stirring for 5 min before measurement. The calorimeter was calibrated electronically. Three lipid systems were used for ITC experiments: POPC/POPG and POPE/POPG (10 mM lipid concentration each) and POPC (20 mM lipid concentration). The LUVs were dispersed in 10 mM Tris buffer containing 150 mM NaCl at pH 7.4. The reaction cell volume was 1.4352 mL. Baseline adjustment experiments were performed by injecting vesicles into the cell containing buffer (blank). Heat flow per injection was corrected by subtracting the blank. Peptides were fully titrated with lipids until no change in the baseline heat profile was observed. In the analysis of ITC data, with the assumption that the peptide interacts with the outer leaflet of vesicles and on the basis of geometric parameters for LUVs, an estimated 50% of the total lipid concentration was used in all calculations.

Fluorescence measurements were performed on a Cary Eclipse fluorometer (Varian). All fluorescence intensities, including those of acrylamide, were corrected for the inner filter effect,[19] and the corresponding blank was subtracted. For Trp fluorescence measurements, excitation wavelength was at 280 nm. Calcein leakage fluorescence experiments were measured with the excitation wavelength at 496 nm and emission wavelength at 517 nm. The total experiment time for each dye-leakage measurement was 15 min with stirring. After 2 min from the start of experiment, the appropriate aliquot of peptide was added and calcein leakage was monitored as the difference from baseline. After 12 min, 100 μL of 20% triton X was added to induce 100% leakage of the dye.

RESULTS AND DISCUSSION

Conformation of HHC-36. Analysis of the concentration dependence of the far-UV CD spectra of HHC-36 in buffer (Figure 1) supports the existence of turn conformations that could be further complicated by the exciton coupling derived from close Trp−Trp interactions in this tryptophan-rich peptide.[20,21] The Trp−Trp exciton coupling has a strength proportional to the rotational strength and separation (in wavelength, $\Delta\lambda$, scale) of the interacting Trp pair.[20] Moreover, the B_b band in tryptophan is centered in the 220−230 nm region.[21] In HHC-36, a nonapeptide with four tryptophan residues, the exciton coupling in the 220−230 nm region can therefore influence the CD spectral features of the secondary structure of the peptide.[22−24]

The CD spectra of HHC-36 in buffer (Figure 1A) also reveal the self-association of the peptide at higher concentrations. The negative molar ellipticity of the peptide increases with concentration until ~100 μM but does not change after this concentration. The self-association of the peptide occurs despite its five positive charges and could be through hydrophobic interactions. Using the ellipticity data at different extrema (205, 214, and 225 nm), a two-state Hill model was applied to the peptide association in the aqueous system. The fitting of the data was not fully consistent with formation of dimers (results not shown); therefore, the existence of higher orders of association could not be excluded. Indeed, peptide trimers ($M_w \approx 4.5$ kDa; M_w of HHC36 is 1488 Da) were detected consistently by SDS-PAGE technique (Figure 1B). In agreement with the CD data, highly intense peptide trimeric bands were detected at 50 and 100 μM concentrations. A faint band was detectable at 20 μM. Despite very faint shadows, bands were not clearly observed for 10 or 5 μM peptide

dx.doi.org/10.1021/jp4096985 | J. Phys. Chem. B 2013, 117, 14697−14708

concentrations. On the basis of CD and electrophoretic data, it is plausible that HHC-36 in aqueous solutions can exist in both monomeric (M) and trimeric (T) forms at equilibrium: $M \rightleftharpoons T$. In the aforementioned two-state model applied to HHC-36 in aqueous solution, regardless of the stoichiometry of self-association, the concentrations of the monomeric and associated forms of the peptide are equimolar at ∼50 μM (i.e., $[M] = [T] \approx 12.5$ μM) (analyzed from CD data in Figure 1). Peptide association could also form amphipathic turn structures with all or some Trp residues internalized and Arg and Lys residues exposed to the aqueous environment, thus maximizing hydrophobic attractive and minimizing charge−charge repulsive interactions. Amphipathic turn structures have been previously reported in other peptides.[25,26] From the CD spectra and SDS-PAGE analysis in Figure 1, it appears that the peptide is monomeric at low concentrations (5−15 μM; no significant change in molar ellipticity and no detectable band in gel electrophoresis chromatogram). The concentration (as well as negative ellipticity and electrophoretic band intensity) of the associated form constantly increases with the increase in peptide concentrations ≥20 μM and reaches a maximum (maximum negative ellipticity/band intensity) at ∼100 μM and above.

To study the stability of the hypothesized turn structure of the nonapeptide against full denaturation in buffer, we measured temperature-dependent CD spectra at 20 μM peptide concentration. The peptide is dominantly monomeric at this concentration, which allows a direct assessment of the stability of its single-stranded form in solution. Figure 2 shows at least

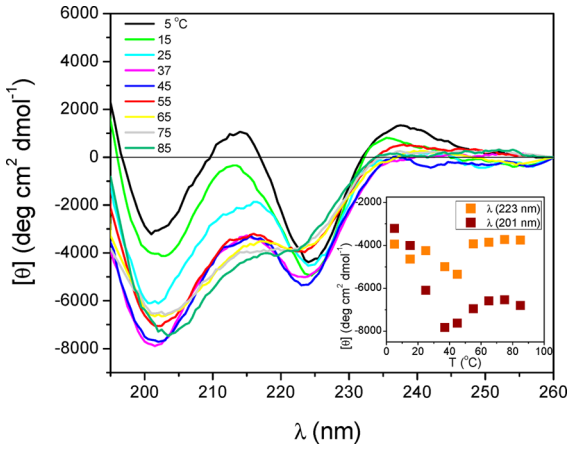

Figure 2. Temperature dependence CD spectra of HHC-36 in buffer at 25 °C. Refer to the Materials and Methods section for experimental details.

two distinct temperature-dependent turn conformations over the temperature range measured. In the 5−45 °C range, the spectra show two negative maximum ellipticities at 201−202 and 223−224 nm. The ratio of the negative maxima ($[\theta]_{201}/[\theta]_{223}$) in this temperature range alters from 0.8 to 1.5, implying a gradual conformational change. A drastic conformational change in the peptide occurs in between 45 and 55 °C (∼50 °C), shown by transformation of the maximum negative ellipticity at 223 to a shoulder-like motif and an increase in the $[\theta]_{201}/[\theta]_{223}$ ratio to ∼1.8.

The conformational change in this wide temperature range (5−85 °C) reveals a possible switch between various turn structures. Therefore, based on the CD information provided in Figure 2 (and inset, which exhibits the change in ellipticity at the two negative maxima, 201 and 223 nm), the combination of these secondary structures can be categorized in two main *average backbone conformations*. The CD spectra also reveal that the peptide backbone does not fully denature at high temperatures and can still possess turn conformations. As previously mentioned, exciton coupling of Trp pairs in close proximity (up to 1.5 nm) can influence the CD spectra of Trp-containing peptides and proteins.[20,23,27] An indication of this influence can be observed in the CD spectra of HHC-36 at low temperatures, 5−15 °C. The positive maxima in the 235−238 nm range, the negative maxima in the 220−225 nm range (which is coupled to the corresponding positive peak at 212−217 nm), as well as the negative maximum at 202 nm imply the presence of Trp−Trp coupled excitons. The minima of the exciton can therefore partially contribute to the overall CD spectra of the peptide at 225 nm (up to 2000 ellipticity units, as exhibited in Figure 2). From the CD spectra in Figure 2, it seems that the influence of the tryptophan exciton coupling on the spectra diminishes at higher temperatures with the decrease in the positive maximum in the 235−238 nm and the corresponding negative maximum in the 220−225 nm ranges.[20] In other words, the influence of Trp−Trp interaction on the peptide structure is more prominent at lower temperatures. The temperature dependence of exciton coupling could be also monitored by the coupled peak ratio at $[\theta]_{215}/[\theta]_{223}$. This ratio is close to 1 at 55 °C, <1 at temperatures <55 °C, and >1 at temperatures >55 °C. As shown in the CD spectra, it appears that the change in exciton coupling is directly related to the change in conformation. Nevertheless, as previously mentioned, the exciton effect on the CD spectra could only partially influence the CD spectra of the peptide, and the peptide's backbone conformation is clearly changed in this temperature range. Overall, the temperature-dependent nature of the CD spectra in HHC-36 can be attributed to at least two distinct interconvertable groups of turn structures (only the average of which can be detected in the CD spectra) stable at low and high temperatures. This observation is further supported by molecular dynamics simulations (see later).

To further understand the influence of Trp exciton couplets observed in the CD spectra, two Trp's (residues 3 and 4) on the N-terminal side of the peptide were singly or doubly substituted by all eight possible combinations of Phe and Tyr residues. It has been reported that the influence of Tyr−Trp, Tyr−Tyr, and Phe−Trp coupling transitions on CD spectrum are not as prominent as the Trp−Trp transition, and the Trp−Trp transition can be detected in the presence of these transitions.[20] In Figure 3A, the CD spectra of W3→F3 (F3) and W4→F4 (F4) analogs are compared with HHC-36. From these spectra, it is apparent that the conformation of the F3 analog is comparable to the original peptide (with only a slight reduction in ellipticity), but the F4 analog shows a different conformation (negative and positive maxima at 202 and 229 nm, respectively).

The spectrum of the F4 analog is very similar to that of HHC-10 peptide, in which Trp7 is replaced by Ile. The subtracted spectrum of the F3 analog from HHC-36 (ΔF_3) is very similar to the spectrum of both peptides, implying that the influence of the substituted Phe on the structure of the peptide is minimal. The subtracted spectrum of the F4 analog from HHC-36 (ΔF_4) is strikingly different from both spectra and is reminiscent of a β-turn of type-B[23] or type-II β-turn.[20,23,27] The ΔF_4 spectrum could be interpreted as the average backbone

dx.doi.org/10.1021/jp4096985 | J. Phys. Chem. B 2013, 117, 14697−14708

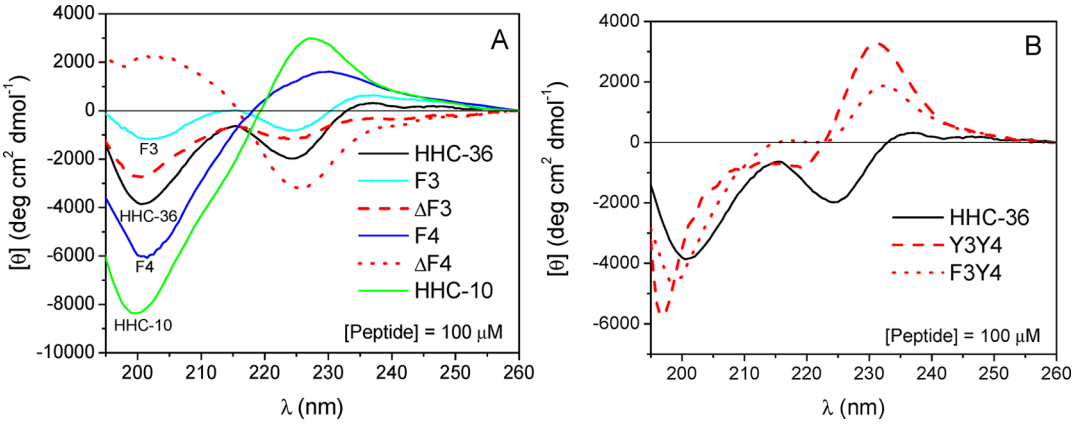

Figure 3. Comparison of the CD spectra of HHC-36 and its aromatic analogs in buffer. (A) CD spectra of HHC-10 and two monosubstituted analogs, W3→F3 and W4→F4, together with their difference spectra from HHC-36, Δ*F*3 and Δ*F*4, respectively. (B) HHC-36 and its disubstituted analogs, W3W4→Y3Y4 and W3W4→F3Y4.

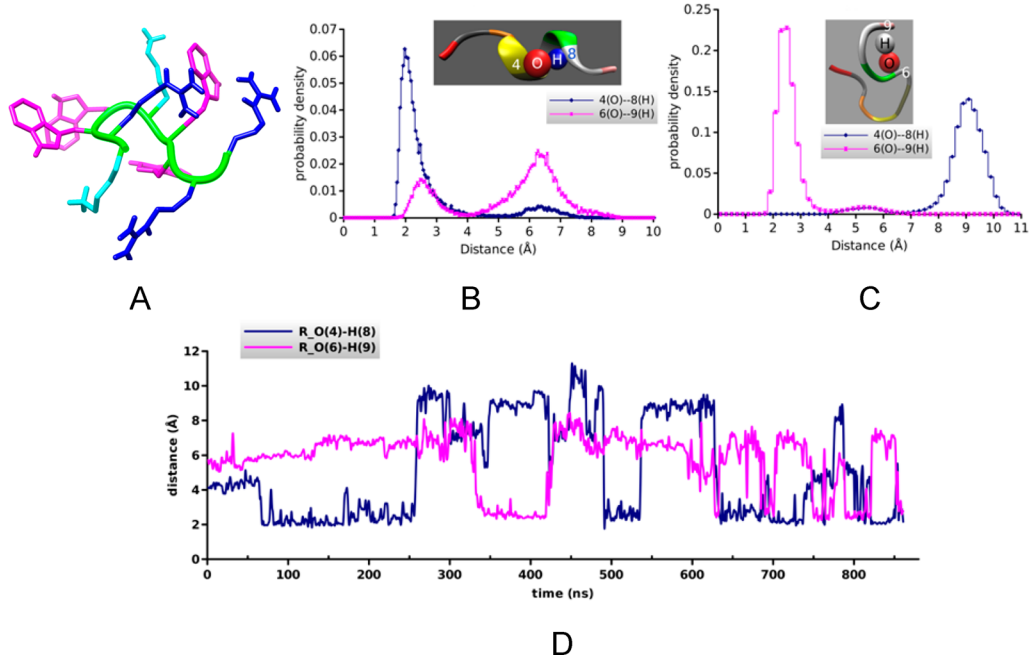

Figure 4. Snapshots of molecular dynamics models of HHC-36 in buffer at 310 K. (A) Snapshot of the dynamic structure of molecule. (B) Probability density distribution for the O···H distance between the respective carbonyl oxygen atoms of residues 4 and 6 and the amide hydrogen atoms of residues 8 and 9 over a time interval of 166.513 ns (1287.128 to 1453.641 ns) of the peptide simulation in aqueous 150 mM NaCl. The inset shows a snapshot of the backbone of the peptide in this time interval with 4(O)−8(H) pair magnified for clarity. (C) Probability density distribution for the same pairs of atoms in panel A with a shorter time interval of 60.532 ns (t = 535.2295 to 595.7615 ns). The inset exhibits a snapshot of the peptide backbone structure during this interval with the 6(O)−9(H) pair magnified for better visualization. (D) Profile of the 4(O)−8(H) and 6(O)−9(H) pairs distances over an interval of 861 ns (from a total of over 1.8 μs) of the peptide simulation in aqueous 150 mM NaCl.

conformation of the HHC-36 peptide in the absence of the exciton couplet. On the basis of this interpretation, the spectrum for the backbone conformation of HHC-36 is distorted due to exciton couplet interference, and this coupling specifically occurs between indole rings of the W4 and W7 residues. The influence of exciton couplets on the CD spectra of the HHC-36 peptide can be further explored by looking into the spectra of its double-substituted analogs, W3W4→Y3Y4 and F3Y4 (Y3Y4 and F3Y4, respectively) in Figure 3B. In both analogs, the CD spectrum of HHC-36 is changed to unique spectra, with respective positive and negative maxima at 231−232 and 197−199 nm. Interestingly, a deflection point at 215−217 nm was observed in the spectra of both peptides, and the coupled extrema, at 216 and 225 nm, in the HHC-36 spectrum disappear. These spectra indicate the blue shift of the negative maximum in HHC-36 from 201 to 199 (in F3Y4) and 197 nm (in Y3Y4). Overall, it appears that simultaneous substitution of W3 and W4 in HHC-36 disrupts the exciton couplet formation between Trp residues and induces more disorder in the peptide conformation (as seen by the negative maximum blue shift).

On the basis of the above arguments, turn conformations can be attributed to HHC-36 in buffer. Transfer of the peptide from buffer to aqueous TFE or PG-containing vesicles (TFE data is not shown; PC/PG data is shown below) results in an increase in the minima at ∼225 nm at the expense of the minima at ∼201 nm. This has been previously reported for indolicidin, which was interpreted as a turn with B-type topology.[21,23,24,28,29] Small-turn peptides containing aromatic side

dx.doi.org/10.1021/jp4096985 | J. Phys. Chem. B 2013, 117, 14697−14708

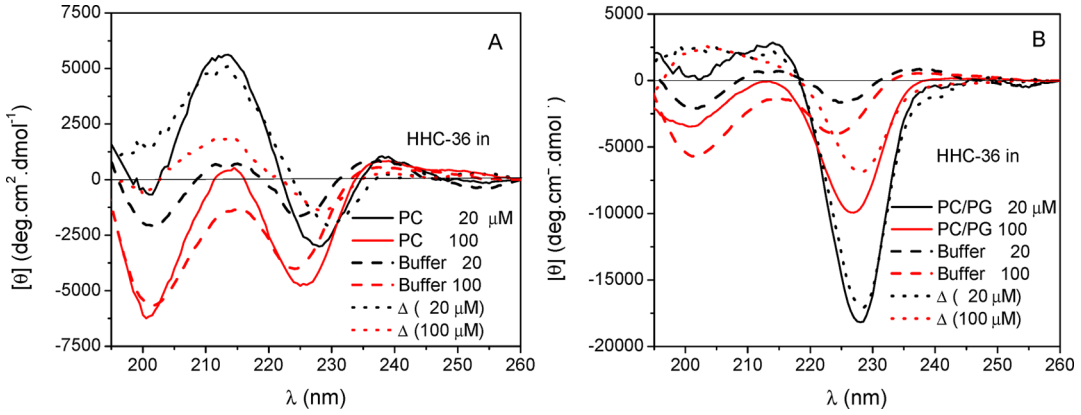

Figure 5. HHC-36 concentration dependence in lipid LUV dispersions in buffer: (A) in POPC and (B) in POPC/POPG (3:1, molar ratio). The difference spectra of the peptide in lipid and buffer systems (lipid-buffer) are shown as Δ([peptide]). Temperature was 25 °C.

chains have been previously reported, albeit most contained the turn-promoting residue, proline, or adopted a *β*-hairpin structures with multiple Trp-containing turns.[23,25,26]

Molecular dynamics simulation studies of the peptide in aqueous solution reveal some insights into the atypical CD spectra of HHC-36. Similar to the CD experiments, molecular simulation results indicate the existence of nonrandom secondary structures in the peptide at 310 K (37 °C) (Figure 4). Results at lower and higher temperatures [278 K (5 °C) and 350 K (77 °C)] suggest that the peptide retains these structures (data not shown). Figure 4A depicts a snapshot of the peptide conformation at 310 K. The sharp and dominant peak of the 4(O)−8(H) pair is consistent with a stable H bond between these residues. The structural turn motifs in the peptide backbone, between residues 4−8, can be attributed to H bonding between residues *i* and *i*+4 (Figure 4B). While the main H bonding occurs between residues 4 and 8, less stable H bonds may also occur between residues 6 and 9 (*i* to *i*+3) (Figure 4C). In the interval shown in Figure 4C, the 6(O)−9(H) pair forms a stable H bond and the 4(O)−8(H) pair does not. On the other end of the molecule (N-terminus), no significant H-bonding interaction occurs between the residues. The MD simulation data also showed a sharp peak at 6 Å in the side-chain center of mass separation frequency histogram for the Trp 4 and Trp 7 side chains. This is consistent with the association of the Trp 4 and Trp 7 side chains via hydrophobic interactions and substantiates the CD experimental results on the possibility of interaction between these two residues (Figure 1S in the Supporting Information).

In Figure 4D, a portion of the time dependence of bond lengths between the carbonyl oxygen 4(O) and the amine hydrogen 8(H) as well as the similar quantity between residue 6(O) and 9(H) are shown. The trace shows rapid (∼10 ns) formation and breakage of these backbone-stabilizing bonds between two states: (1) a "long" state showing slow (∼100 ns) variations in length between 6 and 8 Å and (2) a "short" state showing little variation in length at ∼2 Å. These states have a typical lifetime of ∼100 ns. The plots also show some short-lived (∼20 ns) states of intermediate length (∼4 Å) on the far right of both traces. These rarely occurring states are assumed to be short-lived unstable intermediate states. Other than this small portion of the data on the right, the two states do not coexist; that is, whenever 4(O)−8(H) is "short", 6(O)−9(H) is "long" and vice versa. Taken as a whole, the bond length traces in Figure 4D suggest a competition between two different turn structures: one stabilized by 4(O)−8(H) H bond and the other stabilized by a 6(O)−9(H) H bond. Assuming that H bonding occurs whenever the bond length is <3.0 Å, the fraction of the total time the system spends with the bond length <3.0 Å may be used to estimate the probability of that H bond occurring. Averaging over all the equilibrated simulation data (1234.895 ns), the 4(O)−8(H) H-bonded state was thus found to occur with a probability, P_1 = 0.4934. Similarly the 6(O)−9(H) H-bonded state occurred with probability P_2 = 0.1827. The relative probability can be used to estimate the free-energy difference between these two states of the peptide using: $\ln(P_1/P_2) = (G_2 - G_1)/kT$. This results in an estimate of 0.9932 kT as the free-energy difference with the less probable 6(O)−9(H) bond having the higher energy. This low number, on par with the energy of thermal fluctuations in the system, allows the two structures to coexist at these temperatures. Furthermore, the frequent exchange between the structures, observed during the simulation, suggests that the structure is dynamic, that is, that the two coexisting structures are not energetically isolated from one another. The average lifetime of each state is on the order of 100 ns, giving an exchange rate constant on the order 100 ns^{-1}.Traces of H-bond formation can be observed among other O−H pairs, too, but the 4(O)−8(H) and 6(O)−9(H) pairs are the strongest of all. Results at low and medium temperatures, show similarities with a pronounced turn motif at their N-terminus (data not shown). At high temperatures, the turn motif disappears, but some overall structure is still present that does not represent a fully denatured peptide. These results are in good agreement with the CD thermal analysis in buffer. In that analysis, the conformation of the peptide was transformed in between 45 and 55 °C, and at high temperatures (75 or 85 °C), a considerable decrease in the minimum at 223 nm indicates a decrease in the turn content (Figure 2). Interestingly, in addition to the initially stable 6−9 H bonding (*i* to *i*+3), other stable H-bonding patterns (*i* to *i*+4) emerged between residues 3−7 and 4−8 at longer simulation times (∼1.5 microseconds), which correspond to an *α*-turn motif (Figure 4 and M. Nategholeslam, unpublished results). On the basis of these results, the CD spectra of HHC-36 in aqueous milieu can represent an average of interconvertible dynamic mixture of turn motifs.

Interaction of HHC-36 with Membranes. For a better understanding of interaction of HHC-36 with lipid membranes, conformational properties of HHC-36 in model lipid membranes were studied by CD and fluorescence spectroscopy.

dx.doi.org/10.1021/jp4096985 | J. Phys. Chem. B 2013, 117, 14697−14708

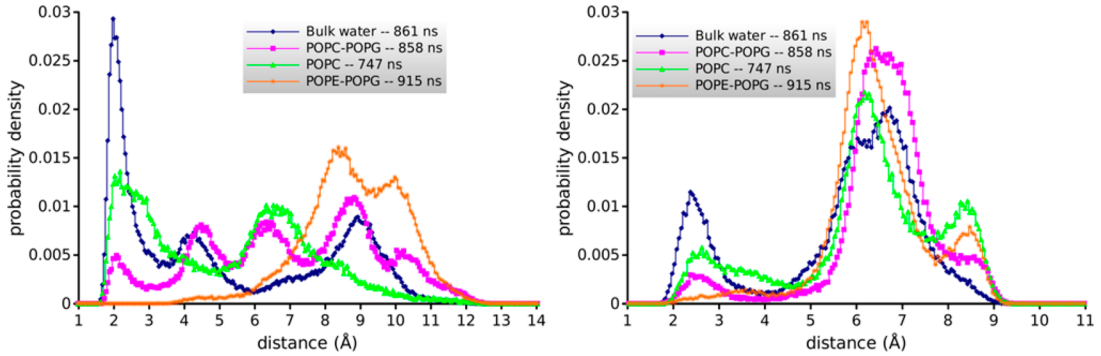

Figure 6. Probability distributions of the (A) 4(O)−8(H) and (B) 6(O)−9(H) atom pair distances in HHC-36 at 310 K in aqueous 150 mM KCl and vicinity of three different lipid model membranes: POPC, POPC/POPG (3/1: molar ratio), and POPE/POPG (3/1: molar ratio). See the Material and Methods section for simulation conditions.

As exhibited in Figure 5, conformation of HHC-36 changes in interaction with model phospholipid membranes representing the mammalian (PC) and bacterial (PC/PG) membranes. CD spectra of the peptide in PC vesicles (Figure 5A) reveal a blue shift at the lower wavelength negative maximum in comparison with the spectrum in buffer. The spectra in PC vesicles are also concentration-dependent and share similar characteristics with the spectra in buffer, retaining a turn conformation. In comparison with the CD spectra in buffer, a pronounced maximum becomes apparent at ∼212 nm that is coupled to the minimum in the 225−230 nm range and is most pronounced at low concentrations and temperatures (Figures 2S and 3S in the Supporting Information). The enhancement of this maximum, coupled to the increase in the negative maximum in the 225−230 nm range, could be due to increased immobilization of Trp's and closer Trp −Trp interactions caused by aqueous−lipid interface partitioning of the peptide into the more hydrophobic core of lipids. The maximum diminishes with increasing peptide concentration, showing a change in the Trp mobility/environment (Figures 5A and Figure 2SA in the Supporting Information). Because the major driving forces for both self-association and membrane interaction are hydrophobic and short-range interactions, increasing peptide concentration that causes self-association (see above) could hinder membrane interaction. A diminishing maximum ∼212 nm coupled to a ∼225 nm minimum, with increase in temperature, in the CD spectra of a predominantly monomeric form of the peptide (20 μM) in PC vesicles further supports this idea (Figure 3SA in the Supporting Information). As depicted by the CD spectra, at low concentration, the conformation of HHC-36 in buffer changes in the presence of lipid, while the spectra at high concentration in buffer and in PC vesicles exhibit comparable conformations. This major conformational difference at low and high concentrations could suggest that the peptide interacts much more strongly with the membrane in its monomeric rather than its associated form. Finally, the difference spectra (shown as Δ in Figure 5A) between PC and buffer indicate the general properties of a β-turn of type B conformation, as previously discussed.

CD spectra in the negatively charged PC/PG system are different from the spectra in both buffer and PC, with a prominently enhanced negative ellipticity and a slight blue shift (compared with buffer and PC spectra) in the 225−230 nm region as well as an essential decrease in the negative maximum at ∼200 nm. Comparable to the PC system, these changes indicate the existence of stable turn structures in the PC/PG system. The maximum negative ellipticity around ∼225 nm shows a constant increase in the 10−35 μM range and then decreases in the 50−125 μM range (Figures 5B and Figure 2SB in the Supporting Information). As with the previous PC case, this observation shows a clear distinction between the membrane interacting properties of HHC-36 at low (primarily monomer) and high (dominantly associated) concentrations. Similar to the PC vesicles, the temperature-dependent CD spectra of the peptide in the PC/PG system (Figure 3SB in the Supporting Information) show a decrease in the extrema at 212 and 225 nm with the increase in temperature. The difference spectra again indicate the general properties of a β-turn of type-B conformation (Figure 5B); however, in this case the maxima of the difference spectra are very broad (between 200 and 215 nm), and the ratio between the maxima and minima is < 1 (in contrast with the same ratio in the PC and buffer difference spectra, which was close to or more than 1). The changes of HHC-36 conformation in buffer and phospholipid milieus are also supported by MD simulations, as shown in Figure 6. The H-bonding pattern in 4−8 (Figure 6A) and 6−9 (Figure 6B) shows a drastic change in the presence of lipids, including the PE/PG system. In the latter system, the strong H bond for the 4−8 pairs in the 2 to 3 Å range fully disappears. As shown in Figure 6, the traces of H bonds between both the 4(O)−8(H) and 6(O)−9(H) pairs are strongest in aqueous solution. These interaction weaken in the presence of lipid (PC, PC/PG, and PE/PG). This might be interpreted as a membrane-induced change in peptide structure, which is most pronounced for the PE/PG membrane and may very well account for part of the entropy contribution to peptide adsorption to this membrane, as observed in the ITC experiments (see below). In addition, the enhancement of the probability density in the 6 to 7 Å and 8 to 9 Å range may point to the influence of Trp−Trp interactions on the peptide structure and its stabilization that requires a more detailed analysis (Figure 1S in the Supporting Information).

We assume that the turn structures of HHC-36 on lipid membranes are related to their molecular forms in the solution. The difference spectra in both lipid systems (PC and PC/PG) could be an indication of a turn conformation, which is further stabilized upon interaction with membranes. The difference spectra could also indicate a net average turn structure with less or no influence from the Trp−Trp exciton interference. This latter speculation is further supported by the difference CD spectra of HHC-36 and its non-Trp aromatic analogs, which

dx.doi.org/10.1021/jp4096985 | J. Phys. Chem. B 2013, 117, 14697−14708

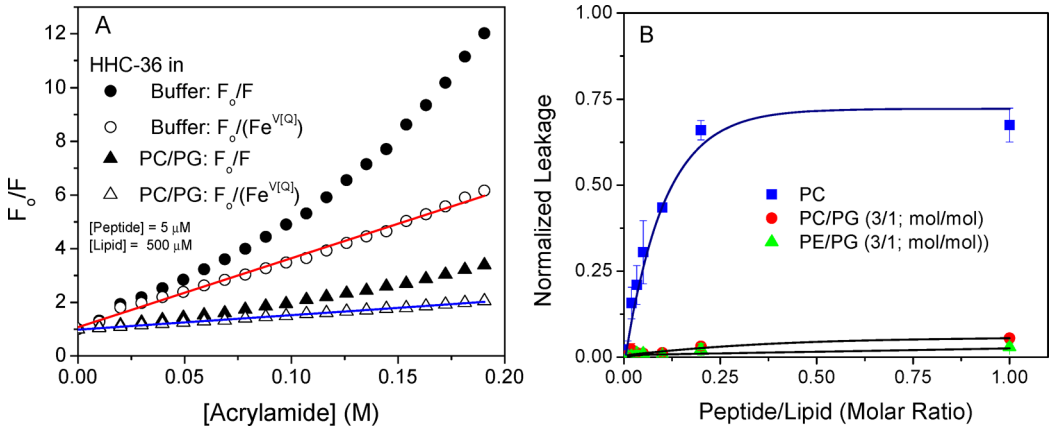

Figure 7. (A) Acrylamide quenching and corrected dynamic quenching of HHC-36 in buffer and PC/PG systems. Linear data represent the contribution of the dynamic quenching and are plotted as $F_o/F^{V[Q]}$ versus [acrylamide]. (See the text for more information.) The peptide/lipid molar ratio was 1/100 ([peptide] = 5 μM). Temperature was 25 °C. (B) Calcein leakage profile of HHC-36 in three lipid systems. The data were recorded for 10 min after the addition of the peptide to lipids. Lipid concentration was fixed to 12 μM. Lipids were dispersed in 10 mM Tris, containing 150 mM NaCl at pH 7.4. Temperature was 25 °C.

indicated a β-turn of type B conformation. (See Figure 4 and the related discussion.)

To further explore the interaction of monomeric HHC-36 with lipid membranes, we studied the degree of tryptophan insertion into the membranes through fluorescence quenching experiments. It is known that acrylamide is an efficient quencher of indole and Trp without penetrating into the lipid bilayers.[30,31] Figure 7A shows Stern–Volmer plots for the acrylamide quenching of HHC-36 in buffer and the PC/PG system. Plots for both systems have an upward deflection, implying the involvement of both static and dynamic quenching mechanisms. It should be also noted that HHC-36 contains four Trps; therefore, the quenching mechanism is complicated. In a typical dynamic quenching process with a single fluorophore type, the Stern–Volmer plot is linear. The dynamic quenching constant, K_D, can be derived as the slope of a linear plot ($(F_o/F) = 1 + K_D[Q]$). In this equation, F and F_o are the respective fluorescence emissions in the presence and absence of the quencher, and [Q] represents the quencher concentration. In Figure 7A, a modified version of the Stern–Volmer equation ($(F_o/F) = (1 + K_D[Q])\cdot e^{V[Q]}$) was used to obtain the linear dynamic quenching component.[30,31] In this modified equation, V represents the volume of the "sphere of action", within which the quencher is adjacent to the fluorophore through a weak interaction at the moment of excitation, acting like a static quencher.[19] As expected, the K_D constant for the peptide monomer in the buffer system (K_D = 25.72) is much higher than all three lipid systems (Table 1). This implies a much higher average accessibility of Trp's to the aqueous environment in the absence of lipids. In the neutrally charged PC lipid system (K_D = 6.81), in comparison with the other two lipid systems, Trp's are less buried and more accessible to the aqueous milieu. The fluorescence emission maximum of the peptide in the PC system is at 349 nm, which is close to the Trp emission in the aqueous environments (typically 350–355 nm) (Table 1). In comparison with other systems, the PC system also has the largest sphere of action volume and radius (V = 4 and R_v = 1.18 nm), indicating that, on average, the Trp's are more accessible (hence, the peptide is less buried) in comparison with negatively charged lipid systems, PC/PG and PE/PG. The fluorescence emission maxima of HHC-36 in both negatively charged PC/PG and PE/PG lipid systems are at 343 nm, which is considerably blue-shifted in comparison with both buffer and PC systems (Table 1). In comparison with the PC system, both dynamic quenching constants (K_D = 5.41 and 6.20; for PC/PG and PE/PG, respectively) and the volume of the sphere of action (V = 3; R_v = 1.06 nm; for both systems) have also decreased, indicating a decreased accessibility of the fluorophore (Table 1). Together, these observations imply a deeper Trp (and peptide) interaction and burial into the interfacial region in the negatively charged lipid systems.

Table 1. Acrylamide Quenching of Trp in HHC-36: Dynamic Quenching Constant (K_D), sphere of Action Volume and Radius (V and R_v, respectively), and Emission Wavelength Maximum (λ_{em})

system	K_D (M^{-1})	V (M^{-1})	R_V (nm)	λ_{em} (nm)
buffer (no lipids)	25.72 ± 0.45	4.03	1.17	352 ± 1
PC	6.81 ± 0.10	4.10	1.18	349 ± 1
PC/PG (3:1)	5.41 ± 0.06	3.00	1.06	343 ± 1
PE/PG (3:1)	6.20 ± 0.14	3.00	1.06	343 ± 1

The calcein leakage assay in Figure 7B shows that the disruption caused by the peptide in the PC system (~75%) is much higher than that caused by both PC/PG and PE/PG systems (<10%). The leakage in the latter two lipid systems is comparable. If we assume that membrane disruption is the main mechanism for the antibacterial activity of this peptide, the dye leakage results will not support the reported biological activity of the peptide against erythrocytes and bacterial organisms, where HHC-36 was found to be only weakly hemolytic with good activity against both Gram-positive and -negative bacteria.[3] The dye leakage results could therefore imply that membrane lysis is not the major or only contributing factor to the biological activity of the peptide. Despite the weak leakage, both negatively charged lipid systems show strong interactions with the peptide, as was revealed from CD and fluorescence spectra as well as ITC measurements (see later). However, it should be noted that peptide binding, while necessary for pore formation (or general membrane disruption) and hence leakage, is not a sufficient condition on its own to ensure leakage. This is clearly shown in more than seven-fold increase in the leakage of the peptide in PC system in comparison with PC/PG and PE/PG systems. A Trp-

dx.doi.org/10.1021/jp4096985 | J. Phys. Chem. B 2013, 117, 14697–14708

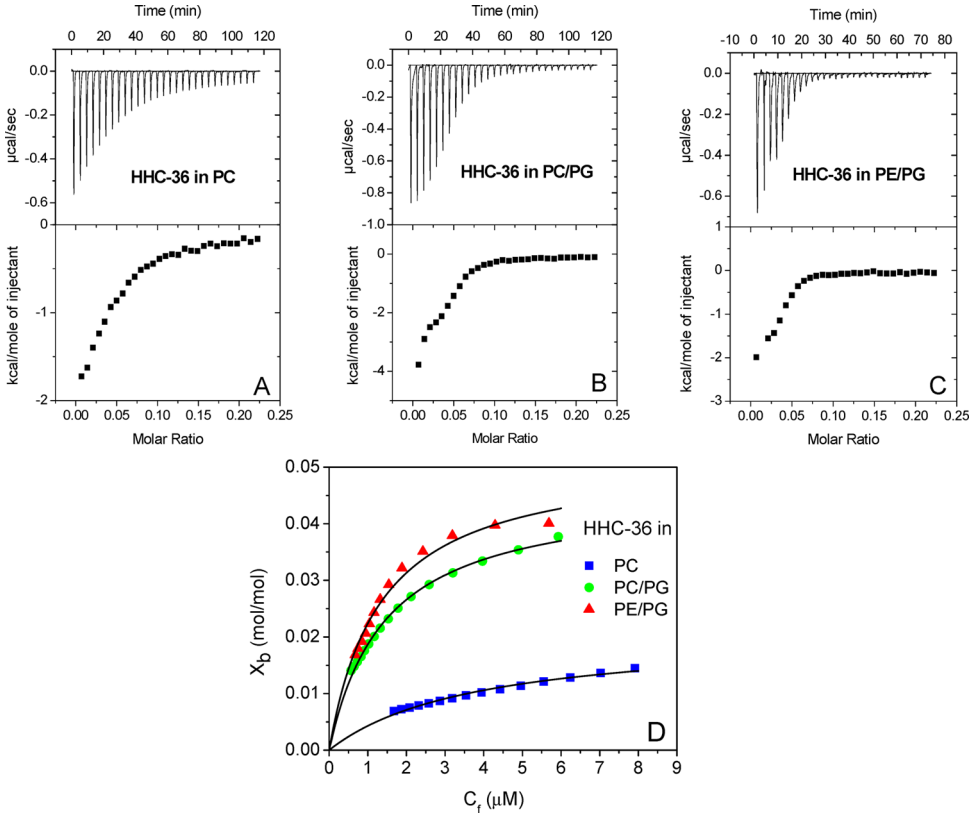

Figure 8. Heat profiles (A–C) and the binding isotherm (D) of HHC-36 in three lipid systems. In these measurements, 10 μM HHC-36 was titrated with lipid LUVs: 20 mM POPC and 10 mM POPC/POPG and POPE/POPG (both at 3:1 molar ratio). Temperature was 37 °C.

Table 2. Thermodynamic Parameters of the Peptide–Lipid Interactions

HHC-36	ΔH_b (kcal·mol^{-1})	B_{max} ($1/B_{max}$) (mol/mol)	K_b (M^{-1})	ΔS_b (cal·mol^{-1}·K^{-1})	ΔG_b (kcal·mol^{-1})
PC	−11.5	0.026 (38.5)	2.6×10^5	−4.3	−10.2
PC/PG	−16.0	0.046 (21.7)	6.9×10^5	−17.1	−10.7
PE/PG	−7.2	0.052 (19.2)	7.5×10^5	11.5	−10.8

containing version of the antimicrobial peptide Gramicidin S, GS10WF,[32] was used as a positive control in all experiments at peptide lipid ratio of 1:5 and 1:50. This peptide strongly interacts with all three lipid systems and is highly hemolytic.

ITC experiments were used to assess the binding affinity of HHC-36 with lipid membranes. The peptide–lipid binding heat profiles and binding isotherms for HHC-36 interactions with the three lipid systems are exhibited in Figure 8A–D. In Figure 8D, X_b represents the degree of peptide binding defined as the moles of bound peptide per moles of lipid, and C_f is the concentration of free peptide in solution. An equilibrium condition is assumed in the binding of peptides to lipid vesicles, and X_b is a function of the free peptide concentration: $X_b = f(C_f)$. The binding isotherms (Figure 8D) suggest that the relation between X_b and C_f is not linear, and saturation sets in at high peptide concentrations.

To calculate the binding constants of HHC-36 for the three lipid systems under equilibrium conditions, we have applied a one-site independent binding partitioning model to the binding isotherms, using the following equation, as previously described:[32]

$$X_b = B_{max}\frac{K_b C_f}{1 + K_b C_f} \quad (1)$$

In this equation, B_{max} is the maximum binding capacity of the peptides to lipid vesicles (in mol/mol or stoichiometric ratio), and K_b is the equilibrium binding (surface partitioning) constant. Note that the only available binding sites are on the outer leaflet of the vesicle, and $1/B_{max}$ represents the average number of lipids per peptide on the outer monolayer of the lipid vesicle. The one-site partitioning model binding curve was fit to the data by Levenberg–Marquardt nonlinear least-squares algorithms to obtain the values for B_{max} (and $1/B_{max}$) and K_b. The calculated K_b values can be used to derive the free energies of binding (ΔG_b) using the following equation:

$$\Delta G_b = -RT\ \ln(55.5K_b) \quad (2)$$

In this equation R is the universal molar gas constant and T is the absolute temperature. The cratic contribution to free energy (~2.5 kcal/mol at 37 °C) is included in this equation by considering the factor 55.5 as the molar concentration of water.[33] Entropy of binding (ΔS_b) was calculated as $\Delta S_b = (\Delta H_b - \Delta G_b)/T$, where ΔH_b is the enthalpy of binding. Table 2 summarizes the thermodynamic parameters of HHC-36 binding to the three lipid systems.

The $1/B_{max}$ values indicate that in the PC system the average number of lipids per bound peptide is approximately two times higher than those for the negatively charged lipid systems. Compared with the neutrally charged PC system, the binding

dx.doi.org/10.1021/jp4096985 | J. Phys. Chem. B 2013, 117, 14697–14708

constants for the PC/PG and PE/PG vesicles are 2.5 to 3 times higher. The effect of the negative charge on the binding constant is comparable for both PC/PG and PE/PG lipid systems and is ∼8% higher for PE/PG vesicles. These parameters imply the important role of the electrostatic interaction of peptides with PG lipids in peptide−lipid membrane binding. The enthalpies of binding of the three systems do not follow a similar trend; in the PC and PC/PG system, ΔH_b increases from −11.5 to −16 kcal·mol^{-1} but decreases to −7.2 kcal·mol^{-1} in PE/PG system. This clearly emphasizes the essential contribution of PC lipids in the HHC-36 binding. The entropy of binding is also different for the three systems. It seems that the role of entropy in the binding of the peptide to PC is not essential (−4.2 cal·mol^{-1}·K^{-1}; $T\Delta S_b$ = −1.3 kcal·mol^{-1}). In the PC/PG system, the entropy of binding is unfavorable (−17.1 cal·mol^{-1}·K^{-1}; $T\Delta S_b$ = −5.3 kcal·mol^{-1}); conversely, the entropy of binding is favorable (11.5 cal·mol^{-1}·K^{-1}; $T\Delta S_b$ = +3.6 kcal·mol^{-1}) in the PE/PG system. ΔG_b, the main parameter for showing the binding affinity (or partitioning) of the peptide, is comparable for all three lipid systems, with a slightly lower value for the PC system [−10.2 (PC), −10.7 (PC/PG), and −10.8 (PE/PG) kcal·mol^{-1}]. Overall, the binding of HHC-36 to all three lipid vesicle systems is enthalpy-driven. The role of entropy is only favorable in the PE/PG system (33% of ΔG_b), which could be partially due to the peptide conformational change (Figure S3 in the Supporting Information) and also the different mode of peptide interaction with this lipid system compared with PC and PC/PG systems. The energetics of binding of HHC-36 to the three lipid systems imply a relatively strong binding affinity, which supports the reported CD and fluorescence studies previously described.

CONCLUSIONS

HHC-36 adopts an unconventional secondary structure in both aqueous and lipid environments. On the basis of the CD spectroscopic and molecular dynamics studies, HHC-36 in aqueous milieus adopts a *dynamic* turn structure, which can be described as a mixture of at least two groups of interconvertible turns (see previous). The formation of these turn structures is driven not only by the formation of intramolecular H bonds but also through interactions of the indole rings of the tryptophan residues (specifically between W4 and W7). In interaction with neutrally and negatively charged lipid membranes, the average turn structure becomes more stable. On the basis of the results of our experimental measurements assisted by MD simulations, this conformation is an average representation of interconvertible turns, more stable than the unfolded state, and not necessarily a stable conventional β-turn.

Concentration-dependent CD and SDS-PAGE experiments show that the peptide self-associates in buffer. Because of the highly charged nature of the peptide, the main drive for self-association is through hydrophobic interactions and stacking of the indole rings of the tryptophans from each peptide monomer. It is highly plausible that to minimize the electrostatic repulsion the positively charged residues are located on the surface of the associated forms of the peptide and the Trp residues are internalized as much as possible. The associated form of the peptide has low affinity for neutrally charged lipid membranes, as revealed by CD spectra (Figure 5A), implying that to interact with and partition into the membrane interface, the peptide monomer should first dissociate from the peptide assembly requiring an input of energy.

HHC-36 interacts with all three lipid systems used in this study and changes its conformation depending on the lipid composition of each system (Figures 5 and 8). This conformational change can be ascribed to stabilization of turn structures resulting from peptide and charged-lipid interactions and from the insertion of Trp residues at the interface of the hydrophobic core of lipid membranes and aqueous environment. The entropy of binding of the peptide for the three lipid systems is revealing (Table 2). Entropy does not play an important role in the PC system (close to zero), is negative in the PC/PG system, and is positive in the PE/PG system. On the basis of these entropies, it appears that the hydrophobic interaction is dominant in the binding of peptides to PC membranes, which can lead to PC membrane disruption (high dye leakage in Figure 7B); negative entropy in the PC/PG system can imply the formation of an organized peptide−lipid complex that can resist the partitioning of the peptide into the hydrophobic core (low dye leakage in Figure 7B); positive entropy in the PE/PG system can imply the formation of an organized peptide−lipid complex that specifically facilitates the partitioning of the peptide in the hydrophobic core of this mixed lipid system and promotes dehydration of interaction surfaces (low dye leakage in Figure 7B). The difference in the interaction of the peptide with the negatively charged lipid systems can be due to the different physical properties and morphology of PC and PE lipids and their mixtures with PG. In general, PE lipids have low tendency to form bilayers, and PE/PG vesicles are smaller than PC/PG vesicles.

It has been previously reported that HHC-36 (and HHC-10) maintain their antibacterial function when fixed on a solid support, with the majority of the peptides showing a quick time release.[34−36] While exhibiting antimicrobial activity against both Gram-negative and -positive bacteria, the densely charged cationic peptide can possibly cross the peptidoglycan layer to reach the bacterial membranes; however, on the basis of this biophysical study, the main mechanism for HHC-36 activity does not seem to be membrane lysis. Nevertheless, the antimicrobial mechanism can still involve a surface-functioning process. It has been reported that the structurally related cationic Trp-containing antimicrobial peptides impair proper cell division through surface-associated mechanisms.[8,9,37] It is also possible that HHC-36 could target specific cell-surface receptor proteins to disrupt their signaling function. This mechanism allows the peptide to exhibit antimicrobial properties at high specificity and low dosage. Another mechanism, possibly less likely, is the internalization of the peptide through a lipid−peptide complex to interact with intracellular anionic substrates such as DNA, RNA, and proteins.

In summary, as a plausible mechanism for the interaction of HHC-36 with lipid membranes, the peptide monomer initially approaches and associates with the membrane surface through long-range electrostatic attraction, followed by the insertion of Trp residues into the interfacial region. Interaction of the peptide with membranes results in changes in peptide conformation. At higher concentrations, the peptide self-associates, and the hydrophobic interaction with membrane interior could be impeded. The monomeric amphipathic peptide can perturb the surface of the zwitterionic PC membranes and cause lysis but does not seem to have strong lytic activity in negatively charged membranes. In comparison with PC membranes, Trp residues are more buried at the

dx.doi.org/10.1021/jp4096985 | J. Phys. Chem. B 2013, 117, 14697−14708

interface of the PC/PG and PE/PG membranes. The proposed mechanism supports an antibacterial mechanism in which the lysis of bacterial membranes is not the main mode of activity for HHC-36.

■ ASSOCIATED CONTENT

Supporting Information

Data to further support the conclusions of this study. The simulated probability distribution of the Trp4−Trp7 distances in HHC-36 at 310 K in the aqueous environment. Concentration-dependent CD spectra of HHC-36 in PC and PC/PG vesicles. Temperature-dependent CD spectra of HHC-36 in PC and PC/PG vesicles. This material is available free of charge via the Internet at http://pubs.acs.org.

■ AUTHOR INFORMATION

Corresponding Author

*Tel: +1-519-884-0710 (ext. 2284). Fax: +1-519-746-0677. E-mail: mjelokhani@wlu.ca.

Present Address

[‖]B.T.: Department of Physics, Capilano University, Vancouver, BC, V7J 3H5, Canada.

Notes

The authors declare no competing financial interest.

■ ACKNOWLEDGMENTS

This work is dedicated to Professor Michio Kondo, in deep gratitude for his mentorship and significant contributions to peptide science. This study was supported by grants from the Canadian Government: CFI to M.J.-N. (6786) and NSERC to M.J.-N. (250119), B.T. (107449), and C.G.G.

■ ABBREVIATIONS:

Fmoc, fluorenylmethoxycarbonyl; HOBt, 1-hydroxybenzotriazole; CD, circular dichroism; DIPEA, *N*,*N*-diisopropylethylamine; DMF, *N*,*N*-dimethylformamide; HCTU, (2-(6-chloro-1*H*-benzotriazole-1-yl)-1,1,3,3-tetramethylaminiumhexafluorophosphate); HOBt, 1-hydroxybenzotriazole; ITC, isothermal titration calorimetry; POPC, 1-palmitoyl-2-oleoyl-*sn*-glycero-3-phosphocholine; POPE, 1-palmitoyl-2-oleoyl-*sn*-glycero-3-phosphoethanolamine; POPG, 1-palmitoyl-2-oleoyl-*sn*-glycero-3-(phosphor-*rac*-1-glycerol) (sodium salt); LUV, large unilamellar vesicle; RP-HPLC, reversed-phase high-performance liquid chromatography; SDS-PAGE, sodium dodecylsulfate-polyacrylamide gel electrophoresis

■ REFERENCES

(1) Spellberg, B.; Powers, J. H.; Brass, E. P.; Miller, L. G.; Edwards, J. E. Trends in antimicrobial drug development: Implications for the future. *Clin. Infect. Diseases* **2004**, *38*, 1279−1286.

(2) Mookherjee, N.; Hancock, R. E.W. Cationic host defence peptides: Innate immune regulatory peptides as a novel approach for treating infections. *Cell. Mol. Life Sci.* **2007**, *64*, 922−933.

(3) Cherkasov, A.; Hilpert, K.; Jenssen, H.; Fjell, C. D.; Waldbrook, W.; Mullaly, S. C.; Volkmer, R.; Hancock, R. E.W. Use of artificial intelligence in the design of small peptide antibiotics effective against a broad spectrum of highly antibiotic-resistant superbugs. *ACS Chem. Biol.* **2009**, *4*, 65−74.

(4) Marr, A. K.; Gooderham, W. J.; Hancock, R. E.W. Antibacterial peptides for therapeutic use: obstacles and realistic outlook. *Curr. Opin. Pharmacol.* **2006**, *6*, 468−472.

(5) Powers, J. P. S.; Hancock, R. E.W. The relationship between peptide structure and antibacterial activity. *Peptides* **2003**, *24*, 1681−1691.

(6) Hancock, R. E.W.; Rozek, A. Role of membranes in the activities of antimicrobial cationic peptides. *FEMS Microbiol. Lett.* **2002**, *206*, 143−149.

(7) Epand, R. M.; Vogel, H. J. Diversity of antimicrobial peptides and their mechanisms of action. *Biochim. Biophys. Acta* **1999**, *1462*, 11−28.

(8) Otvos, L. Antibacterial peptides and proteins with multiple cellular targets. *J. Peptide Sci* **2005**, *11*, 697−706.

(9) Hale, J. D.; Hancock, R. E. W. Alternative mechanisms of action of cationic antimicrobial peptides on bacteria. *Expert Rev. Anti-Infect. Ther.* **2007**, *5*, 951−959.

(10) Brogden, K. A. Antimicrobial peptides: pore formers or metabolic inhibitors in bacteria? *Nat. Rev. Microbiol.* **2005**, *3*, 238−250.

(11) Jelokhani-Niaraki, M.; Ivanova, M. V.; McIntyre, B. L.; Newman, C. L.; McSorley, F. R.; Smith, M. D. A CD study of uncoupling protein-1 and its transmembrane and matrix-loop domains. *Biochem. J.* **2008**, *411*, 593−603.

(12) Pace, N. C.; Vajdos, F.; Fee, L.; Grimsley, G.; Gray, T. How to measure and predict the molar absorption coefficient of a protein. *Protein Sci.* **1995**, *4*, 2411−2423.

(13) MacDonald, R. C.; MacDonald, R. I.; Menco, B. Ph. M.; Takeshita, K.; Subbarao, N. K.; Hu, L.-R. Small-volume extrusion apparatus for preparation of large unilamellar vesicles. *Biochim. Biophys. Acta* **1991**, *1061*, 297−303.

(14) New, R. R. C. *Liposomes: A Practical Approach*; Oxford University IRL Press: Oxford, U.K., 1990.

(15) MacKerell, A. D., Jr.; Feig, M.; Brooks, C. L., III. Extending the treatment of backbone energetics in protein force fields: limitations of gas-phase quantum mechanics in reproducing protein conformational distributions in molecular dynamics simulations. *J. Comput. Chem.* **2004**, *25*, 1400−1415.

(16) Lindorff-Larsen, K.; Piana, S.; Dror, R. O.; Shaw, D. E. How Fast Folding Proteins Fold. *Science* **2011**, *334*, 517−520.

(17) Humphrey, W.; Dalke, A.; Schulten, K. VMD - Visual molecular dynamics. *J. Mol. Graphics* **1996**, *14*, 33−38.

(18) Phillips, J. C.; Braun, R.; Wang, W.; Gumbart, J.; Tajkhorshid, E.; Villa, V.; Chipot, C.; Skeel, R. D.; Kale, L.; Schulten, K. Scalable molecular dynamics with NAMD. *J. Comput. Chem.* **2005**, *26*, 1781−1802.

(19) Lakowicz, J. R. *Principles of Fluorescence Spectroscopy*, 3rd ed.; Springer Science: New York, 2006.

(20) Grishina, I. B.; Woody, R. W. Contributions of tryptophan side chains to the circular dichroism of globular proteins: exciton couplets and coupled oscillators. *Faraday Discuss.* **1994**, *99*, 245−262.

(21) *Circular Dichroism and the Conformational Analysis of Biomolecules*; Fasman, G. D., Ed.; Plenum Press: New York, 1996.

(22) Bush, C. A.; Sarkar, S. K.; Kopple, K. D. Circular dichroism of β-turns in peptides and proteins. *Biochemistry* **1978**, *17*, 4951−4954.

(23) Ladokhin, A. S.; Selsted, M. E.; White, S. H. CD spectra of indolicidin antimicrobial peptides suggest turns, not polyproline helix. *Biochemistry* **1999**, *38*, 12313−12319.

(24) Vass, E.; Majer, Z.; Kohalmy, K.; Hollosi, M. Vibrational and chiroptical spectroscopic characterization of γ-turn model cyclic tetrapeptides containing two β-Ala residues. *Chirality* **2010**, *22*, 762−771.

(25) Cochran, A. G.; Skelton, N. J.; Starovasnik, M. A. Tryptophan zippers: stable, monomeric beta-hairpins. *Proc. Natl. Acad. Sci. U.S.A.* **2001**, *98*, 5578−5583.

(26) Yao, J.; Feher, V. A.; Espejo, B. F.; Reymond, M. T.; Wright, P. E.; Dyson, H. J. Stabilization of a type VI turn in a family of linear peptides in water solution. *J. Mol. Biol.* **1994**, *243*, 736−753.

(27) Arnold, G. E.; Day, L. A.; Dunker, A. K. Tryptophan contributions to the unusual circular dichroism of bacteriophage-Fd. *Biochemistry* **1992**, *31*, 7948−7956.

(28) Deslauriers, R.; Evans, D. J.; Leach, S. J.; Meinwald, Y. C.; Minasian, E.; Nemethy, G.; Rae, I. D.; Somorjai, R. L.; Stimson, E. R.; Vannispen, J. W.; et al. A. Conformation of cyclo(L-Alanylglycyl-ε-

aminocaproyl), a cyclized dipeptide model for a β-bend: synthesis, nuclear magnetic resonance, and circular dichroism measurements. *Macromolecules* **1981**, *14*, 985−996.
(29) Woody, R. W. Studies of Theoretical Circular Dichroism of Polypeptides: Contribution of β-Turns. In *Peptide, Polypeptides, and Proteins*; Blout, E. R., Bovey, F. A., Goodman, M., Lotan, N., Eds.; Wiley: New York, 1974.
(30) Eftink, M. R.; Ghiron, C. A. Fluorecence quenching studies with proteins. *Anal. Biochem.* **1981**, *114*, 199−227.
(31) Jelokhani-Niaraki, M.; Nakashima, K.; Kodama, H.; Kondo, M. Interaction and orientation of an α-aminoisobutyric acid- and tryptophan-containing short helical peptide pore-former in phospholipid vesicles, as revealed by fluorescence spectroscopy. *J. Biochem.* **1998**, *123*, 790−797.
(32) Jelokhani-Niaraki, M.; Hodges, R. S.; Meissner, J. E.; Hassenstein, U. E.; Wheaton, L. Interaction of gramicidin S and its aromatic amino-acid analogs with phospholipid membranes. *Biophys. J.* **2008**, *95*, 3306−3321.
(33) Cantor, C. R.; Schimmel, P. R. *Biophysical Chemistry, Part I*; Freeman: New York, 1980.
(34) Kazemzadeh-Narbat, M.; Noordin, S.; Masri, B. A.; Garbuz, D. S.; Duncan, C. P.; Hancock, R. E. W.; Wang, R. Z. Drug release and bone growth studies of antimicrobial peptide-loaded calcium phosphate coating on titanium. *J. Biomed. Mater. Res., Part B* **2012**, *100B*, 1344−1352.
(35) Gao, G. Z.; Lange, D.; Hilpert, K.; Kindrachuk, J.; Zou, Y. Q.; Cheng, J. T. J.; Kazemzadeh-Narbat, M.; Yu, K.; Wang, R. Z.; Straus, S. K.; et al. The biocompatibility and biofilm resistance of implant coatings based on hydrophilic polymer brushes conjugated with antimicrobial peptides. *Biomaterials* **2011**, *32*, 3899−3909.
(36) Kazemzadeh-Narbat, M.; Kindrachuk, J.; Duan, D.; Jenssen, H.; Hancock, R. E. W.; Wang, R. Z. Antimicrobial peptides on calcium phosphate-coated titanium for the prevention of implant-associated infections. *Biomaterials* **2010**, *31*, 9519−9526.
(37) Rosenberger, C. M.; Gallo, R. L.; Finlay, B. B. Interplay between antibacterial effectors: A macrophage antimicrobial peptide impairs intracellular Salmonella replication. *Proc. Natl. Acad. Sci. U.S.A.* **2004**, *101*, 2422−2427.

■ NOTE ADDED AFTER ASAP PUBLICATION

This paper was published ASAP on November 18, 2013. The Supporting Information paragraph in ASSOCIATED CONTENT was updated. The revised paper was reposted on November 27, 2013.